Hindawi
Advances in Civil Engineering
Volume 2021, Article ID 5584229, 17 pages
https://doi.org/10.1155/2021/5584229

Research Article

Study of Electric Field Impact on Crystallization in Tunnel Drainage Pipes in Hard Water Area

Liangwen Wei,[1] **Jingyi Guo**,[2] **Xuefu Zhang**,[1] **Yunqi Li**,[3] **and Peng Huang**[1]

[1]*State Key Laboratory of Mountain Bridge and Tunnel Engineering, Chongqing Jiaotong University, Chongqing 400074, China*
[2]*School of Foreign Languages, Chongqing Jiaotong University, Chongqing 400074, China*
[3]*T. Y. Lin International Engineering Consulting (China) Co., Ltd., Chongqing 401121, China*

Correspondence should be addressed to Liangwen Wei; weiliangwen@163.com

Received 25 February 2021; Accepted 12 June 2021; Published 30 June 2021

Academic Editor: Francesco Colangelo

To solve the problem of blockage of crystallization in tunnel drainage pipes in hard water area, electric field devices are designed and applied in the transversal tunnel drainage pipe according to the fundamental law of crystallization. Laboratory tests were carried out to test the crystallizing tunnel drainage pipe under the effect of electric field in order to study the law of electric field impact on crystallization in tunnel drainage pipes in hard water area. The test results indicate that the arranged circumferential and parallel plate electric field devices can form an electrical field within a narrow and small space inside the pipe and influence the ion movement in water and adsorption performance between crystals and the pipe. Under the condition of full flow, the amount of crystals in the ordinary pipe without electric field treatment increases progressively along water flow direction and remains relatively uniform later. The amount of crystals along the water flow direction of the pipe treated with circumferential and parallel plate electric fields presents signs of fluctuation in the early stage and then stableness later. The amount of crystals in the fluctuating section is higher and lower in the uniform section, and its uniform section length is longer than that in ordinary pipes. Under the condition of full current, crystallizing speed declines with elapse of running time. After the electric field is imposed, crystallizing acceleration progressively decreased to a relatively lower level. Comparing three voltages of 5 V, 12 V, and 24 V, the effect of scale inhibition under 5 V is superior. When water amount in the pipe varies, the effects of scale inhibition under different electric field modes are different. The electric field effect causes the changes of the external form of calcium carbonate crystal and its surface abrasion, porous crystal, and structural looseness.

1. Introduction

With the development and expansion of tunnels and underground works, construction tunnel illness and damages are appearing progressively in construction and operation stages. In hard water areas, due to greater calcium and magnesium ion concentration in water after they contact the carbon dioxide in air, crystals are formed and adhere to the inner wall of the tunnel drainage pipe which further causes narrowing of flow diameter of the pipe, thus resulting in the blocked pipe for a long time. The blockage of drainage pipe may lead to cracking lining or leakage. Figures 1 and 2 show the crystal blockage in the tunnel in the ring line section of the Chongqing Municipal Rail Transport. Such solutions to similar problems in oil refinery and sewage treatment works have been found. However, a study needs to be conducted whether such scale inhibition and scale removal methods can also be applied to the tunnel drainage system and whether they can fulfill the purpose of scale inhibition and scale removal in the tunnel drainage system. Due to the fact that drainage pipes in the tunnel system are arranged everywhere and transverse drainage pipes of central drainage are arranged once the pipes are blocked, it is difficult to handle that will make normal drainage impossible or failure. Thus, the function of the tunnel drainage system fails. For the purpose of this problem, we can only increase the diameter of the drainage pipes to solve the blockage, but this solution is only a temporary relief, not a permanent solution.

Figure 1: Tunnel pipe blockage in the section between North Station and Yulu Station.

Figure 2: Tunnel pipe blockage in the section between Danzishi Station and Tushan Station.

Currently, many achievements in the study regarding calcium carbonate crystallizing and electric field water have been attained. Zhuge et al. [1] investigated the superfine calcium carbonate crystallizing process in a test study. Luo et al. [2] discovered in their study that magnetic treatment may inhibit the generation of calcium carbonate crystals. Xiao et al. [3] derived a model on carbonate scaling inside the tunnel pipe using classical ion theory. Vetter [4] studied the mechanism of and influences on barium sulfate scaling. Moghadasi [5, 6] investigated and studied the calcium sulfate and calcium carbonate scaling process in combination with crystal growth theory and in-house test. Tore [7] studied the mechanism of calcium carbonate crystallizing through laboratory rock core flow test. Salima et al. [8] studied the submarine well equipment through dynamic testing and analyzed the calcium carbonate and barium carbonate scaling situations. Viles [9] made a relatively complete summary of the studies on carbonate depositions such as calcium made by countries in the past 100 years.

Lu [10] studied the calcium carbonate deposits in different hydraulic states. Yang [11] summarized calcified deposits mechanism and influences. Tang [12] placed perfluorinatedsulfonic acid resin dispersion, a scaling inhibitor agent on the inner wall of pipes to test study the method of reducing hardness of water. Chen [13] applied PHREEQC, the simulating software, to analyze the influences on calcium sulfate dehydrate crystals. Chen [14] et al. pointed out that after water enters the high-frequency electric field, water molecules may polarize and reduce scaling absorption ability. Xue [15] pointed out that high-frequency electric field may increase the electronegativity of salt crystals in solution. Wang [16] studied the intensified heat transfer of high-pressure static scale resistance through static and dynamic tests. Li et al. [17, 18] analyzed the calcium carbonate crystallizing process and crystal features by the static electric field. Wu [19] studied the scale resistance effectiveness of the combined effect of the homopolymer of itaconic acid (PIA) and the high-pressure electric field. Wang et al. [20] studied the dispersion coefficient and circumferential distribution factor of the irons in calcium carbonate aqueous solution. Li et al. [21] monitored the conductivity in the solution and studied the influences of static electric field on the calcium carbonate crystallizing process. Liu et al. [22] placed cooling circulating water of power station in the self-made "high-pressure static electric water treatment device" to study dynamic simulating scale inhibition. Yuan [23] et al. made a static coupon test and found that the scale inhibition effect declines with an increase in total hardness of water. Cai [24] treated water by the high-frequency electric field and found that scale inhibition is inclined to reduce with an increase of calcium ion concentration. Li et al. [25] carried out a scale inhibition test using circulating water with high hardness and alkalinity to study the influence of electric pressure on scale inhibition result.

To solve the problem of crystal blocked transverse drainage pipes in the tunnel, this paper conducted a study on the law of crystallization in tunnel drainage pipes in hard water areas in accordance with the crystallization mechanism of tunnel drainage pipes in hard water areas by designing an electric field testing device.

2. Test Device and In-House Test Solution

2.1. Principle of Crystallization. Due to the fact that a considerable amount of calcium and magnesium ions and carbonate radical irons exists in groundwater in hard water areas, and they provide basic elements to generated calcium carbonate crystals and magnesium carbonate ions. According to the basic laws of crystal dynamics, the crystals generate in three major steps [26]. In the first stage, the scale ions in the solution are carbonate magnesium ions and carbonate radical ions that are in a saturated state. In the second stage, the crystal core forms, and in the last stage, the crystal grows up. After the above three conditions are met in the tunnel drainage pipes, the following chemical reactions may occur:

$$\begin{aligned} Ca^{2+} + HCO_{3^-} &\longrightarrow CaCO_3\downarrow + CO_2\uparrow + H_2O \\ Mg^{2+} + HCO_{3^-} &\longrightarrow MgCO_3\downarrow + CO_2\uparrow + H_2O \\ MgCO_3 + H_2O &\longrightarrow Mg(OH)_2\downarrow + CO_2\uparrow \end{aligned} \quad (1)$$

Since calcium carbonate, a salt which hardly dissolves, may cause over saturation in local areas of tunnel pipe surface, the crystals from the solution may deposit on the wall of the pipes and finally form calcium carbonate crystals. After the electric field is imposed, the total energy in the

solution increased under the electric field effect. Then calcspar can receive sufficient energy and transforms to other amorphous vaterite such as metastable crystalline phase by reverse reaction [27].

In those relevant tunnel projects in Chongqing and Guizhou, abundant calcium ions and bicarbonate radicals exist in water and the test ions Ca^{2+} and HCO_3^- were chosen as solutes, which meet the definition of hard water as well. However, due to the poor stability of analytically pure calcium bicarbonate, it cannot be used in the test. Hence, analytically pure calcium chloride ($CaCl_2$) as a test solution and analytically pure sodium bicarbonate ($NaHCO_3$) are used to prepare the test solution [28].

2.2. Design of the Electric Field Device. According to the crystallization principle and engineering practice, safety of running vehicles and people in the tunnel environment shall be safeguarded. Hence, a type of low pressure and higher electric field device shall be provided, and by this device, a stable electric field can be formed inside the pipe and drive electric ions to move to poles in the water flowing process. Hence, my design team designed two types of testing devices that can form stable electric field to act on cross-drainage pipes in the tunnel.

The abovementioned testing devices are circumferential and parallel plate electric field devices, respectively, which were designed by roughly identical design principles. Metal appliances in transformer connections were applied in both devices. Positive and negative electricity were imposed, respectively, to distribute electric charge on the metal materials, thus forming an electric field as shown in the schematic drawings in Figures 3–6.

The circumferential electric field device consists of a direct current transformer transformed from alternating current, steel plastic compound pipe ($R = 32$ mm, metal lining, and PVC layer), hard-type fine metal rod sleeve and twisted pair, etc. The alternating current is transformed into direct current by the transformer, and the two output ports are connected to the metal pipe of steel-plastic composite pipe and core hard-type guideline, which is isolation-treated. When power current is on, a radial electric field will form inside the pipe. When the ions are driven to move in the electric field under the action of the electric field, the positive and negative ions are separated.

The parallel plate electric field device is made up of the direct current transformer transformed from alternating current, two pieces of completely identical metal sheet, and PVC pipes ($R = 32$ mm). This device needs to be laid out at the top and the bottom of a pipe, thus forming a parallel vertical electric field mode between the two metal sheets. After the two metal sheets are isolation-treated with insulating cement, they are connected to two output ports of the direct current transformers to make these two metal sheets charged with electricity and an electric field generated between the two metal sheets.

By these two solutions, the positive and negative electric charges distribution, voltage size may be adjusted according to variation of test plan so as to change electric field strength and its direction.

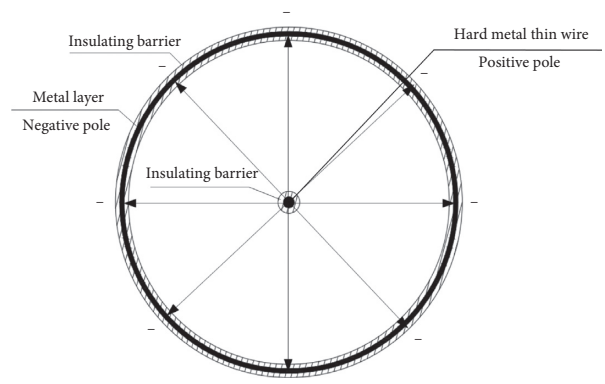

Figure 3: Indicative sketch of the cross-section of circumferential electric field device (center anode).

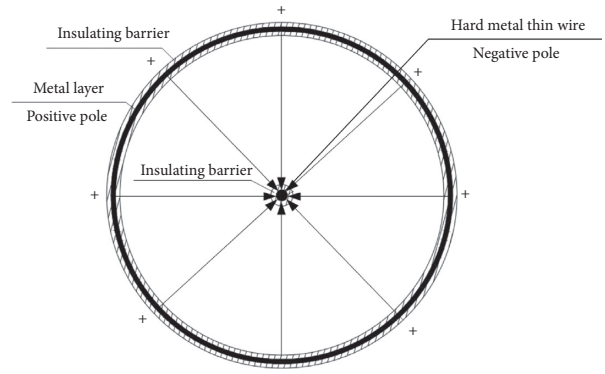

Figure 4: Indicative sketch of the cross-section of circumferential electric field device (center cathode).

2.3. Test Solution. In this paper, the focuses of study are laid on the under the action of electric field and conditions of full current, the tunnel crystal axial distribution, crystal weight, and speed as well as the influences on the crystal weight affected by tunnel electric field mode and electric field line directions under semi-flow condition. The relevant control parameters in the test are shown in Table 1.

2.3.1. Test on Axial Distribution Law of Drainage Pipes. By analyzing the axial distribution law of crystal substance, the position of generating crystals in the pipes can be found that helps solve the crystal blockage problem. By weighing the mass of calcium carbonate crystals in the pipe, the crystal axial distribution situation inside the pipe can be studied by its mass distribution. The pipe crystal conditions are greatly affected by time. In order to safeguard the more stable axial distribution of crystals in the pipe, the test data obtained after 50 days of running are chosen for analysis, and after the end of the test period, the dry weight of the pipe is obtained by oven-drying method.

In order to impede direct contact between calcium ions and pipe wall to avoid adhesion of crystals, it was selected that electric field points to circle center in the circumferential electric field, while the electric field is arranged from bottom to top in the parallel electric field. The test

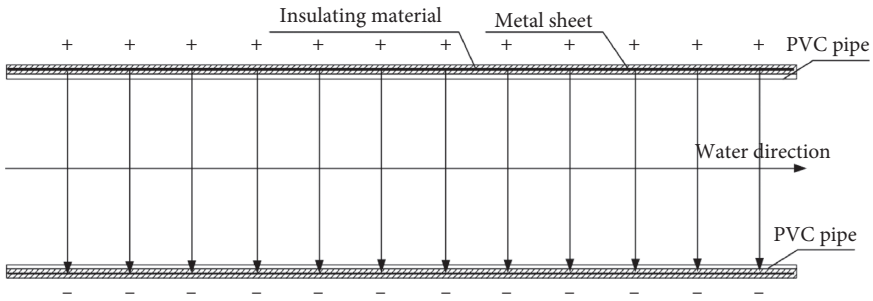

Figure 5: Indicative sketch of the longitudinal section of parallel plate uniform electric field device (anode of the top plate).

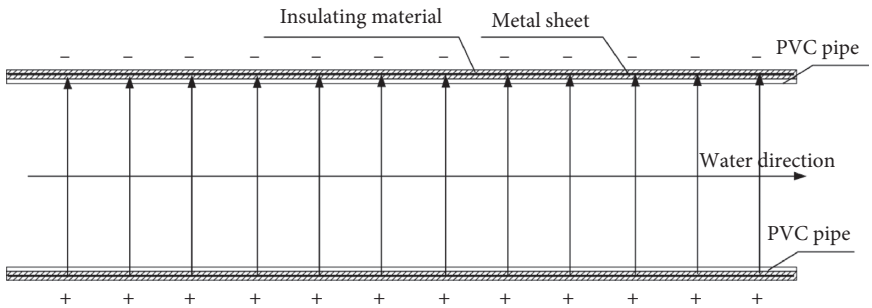

Figure 6: Schematic drawing of the longitudinal section of parallel plate uniform electric field device (anode of the bottom plate).

Table 1: Summary of test parameters.

Test control items	Control parameter
Pipe length	1.2 m
Current speed in pipe	0.68 m/s (full-current) 0.3 (semi-current)
Output voltage	5 V/12 V/24 V
Current state inside pipe (CO_2contact areas)	Full-/semi-current
Slope gradient	0 (not set)

parameters chosen in the axial distribution law test are shown in Table 2.

The schematic drawing indicating the testing pipe layout is shown in Figure 7.

2.3.2. Test on Scale Resistance Effect of Electric Field of Full- and Semi-Flow Pipes. By theoretic study and documentation records, electric field generates active positive impacts on scale resistance, but such application in the tunnel engineering field has been rarely studied. In our test, two types of electric fields, namely circumferential electric field and parallel plate electric field simulation tests, were carried out. The scale inhibition effect of electric fields in conditions of full- and semi-flow is mainly evaluated by contract analysis of tunnel crystal amount, crystallizing speed, scale inhabiting rate, and crystal features. To study crystallizing speed, five testing periods are used in the whole test with each period running for 10 days. The parameters used in the test are consistent with the study of axial distribution law.

Table 2: Summary of testing parameters of axial distribution law of pipe crystals.

Test control item	Control parameters
Lab temperature	25°C
Single pipe length	10 cm
Pipe quantity	12 sections
Current speed in pipe	0.68 m/s
Output voltage	5 V/12 V/24 V
Electric field direction	Radial to circle center (circumferential field) Bottom to top parallel type (parallel plate field)
Pipe inside flow status (CO_2touch areas)	Full-flow status (ideal touch areas of 0)

The test device in the situation of full flow is similar to that of the axial distribution law test whose parameters are shown in Table 3.

In dry season, a small amount of water is inside the pipe, calcium ions and the like have a large touching area with air, and the chance of forming calcium salt also increases that further intensifies the pipe blockage. The semi-flow form is used to simulate the crystallization inside the pipe in dry seasons.

In dry season, under circumferential electric field mode, if electric field direction presents radial pattern pointing to the wall of the pipe, the positive ions (red circle) such as calcium and bicarbonate ions (green circles) may distribute in the manner shown in Figures 8 and 9 (only indicative figures, not representing reality distribution law of ions in solution). If the electric field direction is a radial pattern

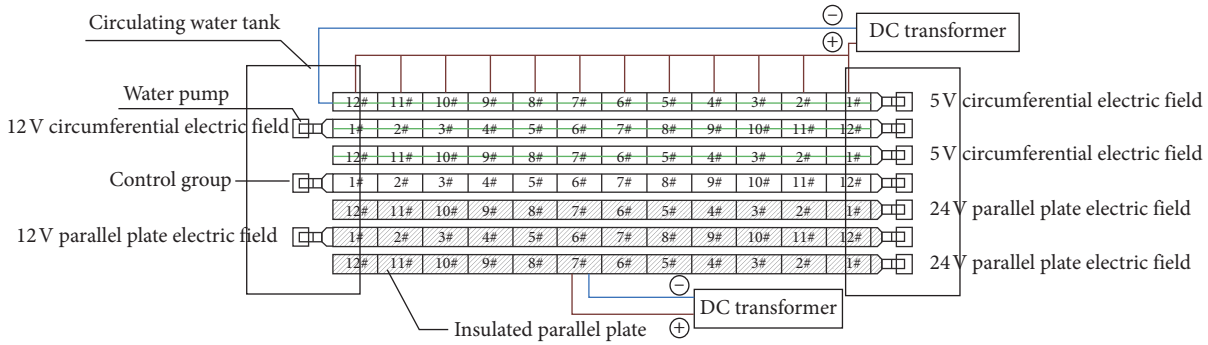

Figure 7: Schematic drawing of the test device indicating axial distribution law of pipe.

Table 3: Test parameters indicating electric field impact on scale inhibition effect of the full-flow pipe.

Test control item	Control parameters
Lab temperature	25°C
Single pipe length	120 cm
Flow speed in the pipe	0.68 m/s
Output voltage	5 V/12 V/24 V
Electric field direction	Radial to circle center (circumferential field) Bottom-to-top parallel type (parallel plate electric field)
Flow status in pipe (CO_2touch areas)	Full-flow state (ideal touch area of 0)

pointing to the center, the distribution of anode ions are the states indicated in the figures. The figures show that when the calcium ions gather on the wall of the pipe, only both ends of liquid level contact air. When the calcium ions are attracted by the center conductor, calcium ions gather at the center of liquid level, and the area of contact with CO_2in the air increases. By the same token, under the condition of the parallel electric field in dry season, if the electric field is changed the cations and anions, the distribution state will be different as shown in Figures 10 and 11. Hence, based on the four situations of the electric field line under semi-flow conditions in Figures 8 to 11 A, B, C, and D, the four groups of DC 12 V are considered, which are applied to the rest of other parameters and full-flow conditions as well.

The overall test device is shown in Figure 12.

2.4. Calculation of Crystallizing Speed and Scale Inhibition Rate. In the process of crystallization, different crystallizing rates are proposed according to the increment of crystals in the pipe in each period.

$$v = \frac{m_n - m_{n-1}}{T}, \tag{2}$$

where $m_n$is the pipe crystal weight after the period n (g), $m_{n-1}$is the pipe crystal weight after period $n-1$(g), and $T$is the test period (d).

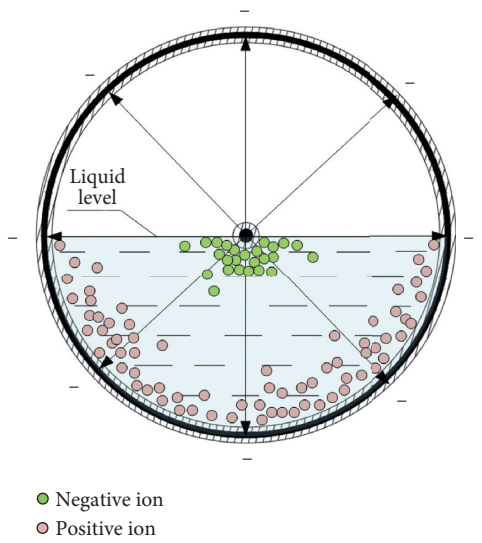

Figure 8: Circumferential: out to inside (group A).

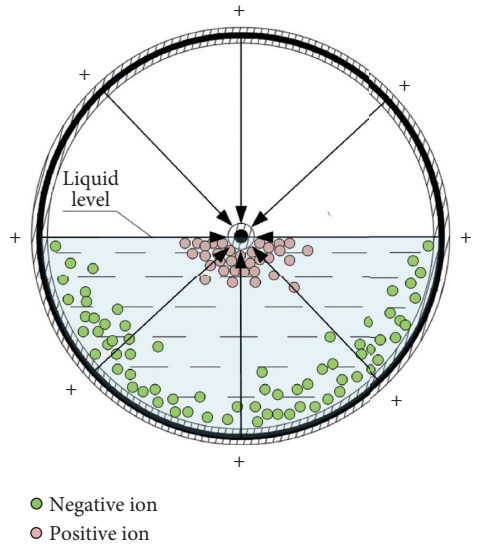

Figure 9: Circumferential: inside to outside (group B).

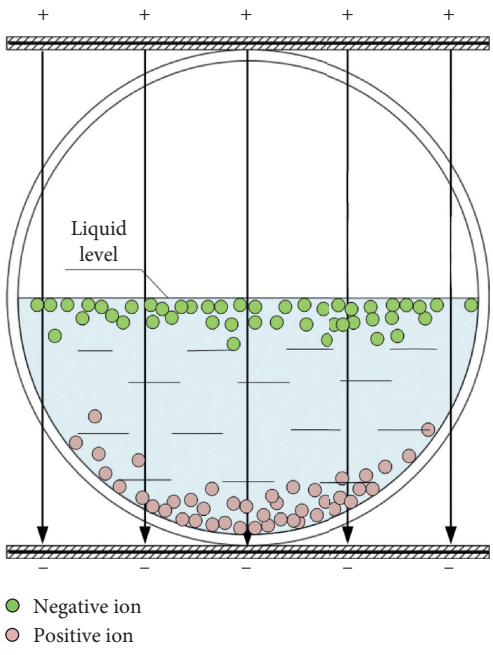

Figure 10: Parallel plate: top to bottom (group C).

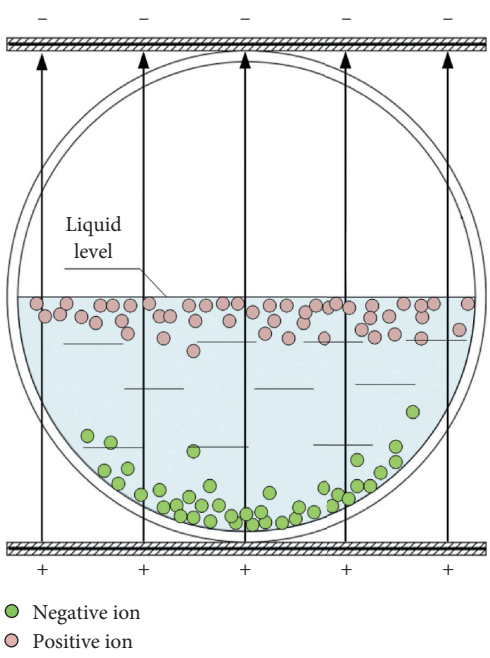

Figure 11: Parallel plate: bottom to top (group D).

In the test, pipe weight is weighed to determine the weight of the crystal substance and analyze the scale resistance rate $\eta$of the tested pipe as follows:

$$\eta = \left(1 - \frac{m_1}{m_0}\right) \times 100\%, \tag{3}$$

where $m_1$is the crystal weight of tested pipe (g) and $m_0$is the weight of empty pipe in comparison with pipe with crystal (g).

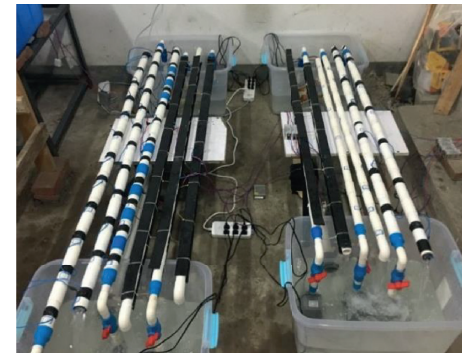

Figure 12: Indicative sketch of the whole test device.

3. Lab Test Results and Analysis

3.1. Analysis of the Law of Crystal Axial Distribution of the Drainage Pipe. For purpose of analyzing the law of pipe crystal axial distribution influenced by electric field, first, the pipe crystal axial distribution without electric field needs to be understood. Meanwhile, the pipe crystal axial distribution situation imposed with the circumferential and parallel plate electric fields should be analyzed. The test schemes are mentioned above. The actual pipe arrangement during the test running period is shown in Figure 13. Pipes 1# to 12# are pipe numbers arranged in order from the outlet port of the pump to the rear end of the pile along the axial direction of the pipe.

When the electric field is not imposed, the crystal amount of all the pipes is plotted into axial distribution lines; thus, the axial distribution of pipe crystals is obtained as shown in Figure 14.

The figure above is the pipe crystal axial distribution curve without an electric field after running for 50 days. The curves directly show the pipe axial distribution law, and one can roughly see that crystal amount increased progressively along water flow direction and then remained stable to a certain degree. The figure also shows that in the ordinary and common pipes after running for 10 days, the minimum crystal amount in the pipe is 0.42 g, and at the inlet port of the pipe, the crystal amount increased progressively along the water flow direction. The crystal amount of each pipe section was not stable until reaching pipe 6# where the crystal amount was almost stable and kept around 0.68 g. The crystal amount reached the maximum at the outlet port of pipe 12# in the amount of 0.71 g.

In the following part, the two types of electric field patterns namely the circumferential electric field pattern and parallel plate electric field pattern test results are described. The pile crystal axial distribution law is obtained by axial distribution curves that help us observe the crystal distributions.

After circumferential electric field treatment and in combination with axial distribution curves of ordinary pipes untreated with the electric field, the crystal axial distribution curves of all pipes are obtained as shown in Figure 15.

(1) After the test running for 50 days under the pressure of 5 V, the maximum value of crystal amount in the

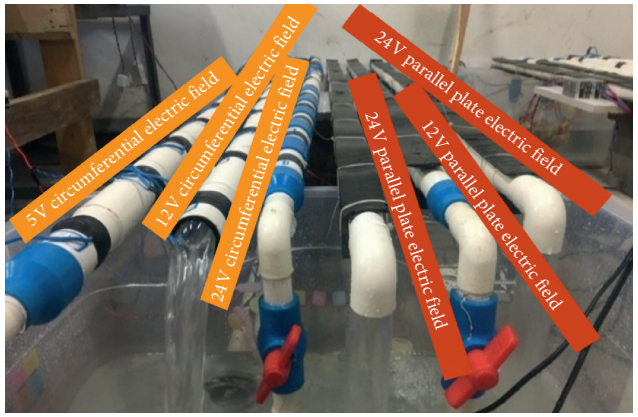

Figure 13: layout of pipes in test running period.

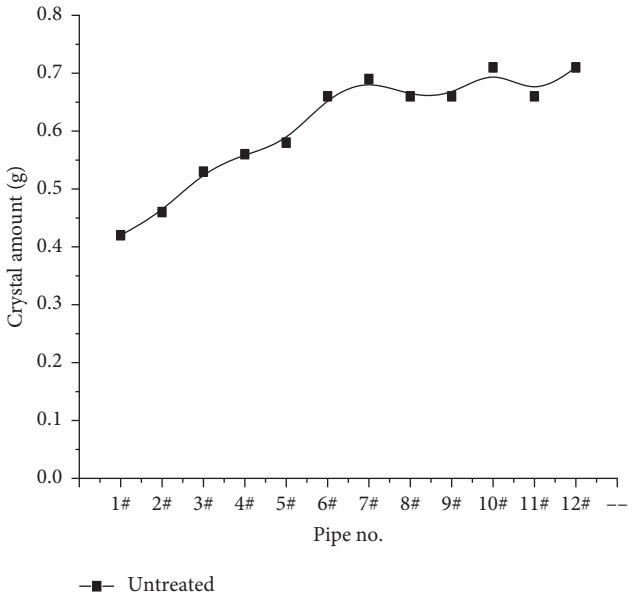

Figure 14: Curves of axial distribution of crystal amount in ordinary PVC pipe untreated with the electric field.

pipe was 0.45 g, which was located in pipe 12#; Under the pressure of 12 V, the maximum value of crystal amount was 0.48 g, which was located in pipe 4#; Under the pressure of 24 V, the maximum value of crystal amount was 0.64 g, which was located in pipe 12#.

(2) After circumferential electric field treatment, the overall pipe crystal amount was less than the crystal amount in the pipe without electric field treatment. However, in the four tests, the crystal amount difference between pipes 1# and 2# was small.

(3) The crystal amount distribution at pipe entrance was not uniform no matter the output voltage of the electric field was 5 V, 12 V, or 24 V.

(4) The crystal axial distribution curve is of a certain relationship with voltage values. The figures show that the crystal amount is minimum under the effect of 5 V at the middle section of the pipe while the crystal amount is slightly higher than the crystal amount under voltage 12 V. The crystal amount under 24 V is higher than the crystal amount of pipes under other different voltages.

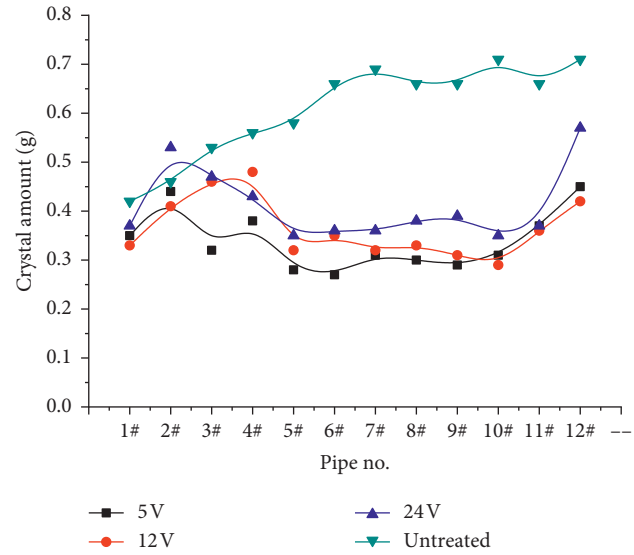

Figure 15: Circumferential electric field mode and corresponding group pipe axial distribution curve.

After treatment with parallel plate electric field, the crystal amounts of all pipes are plotted into axial distribution curves, and in combination with the axial amount, distribution curves of ordinary pipes without treatment of electric fields Figure 16 are obtained.

The following can be seen from the figure:

(1) After test running for 50 days, the maximum values were obtained: 0.41 g under 5 V in pipe 12#, 0.58 g under 12 V in pipe 4#, and 0.54 g under 24 V in pipe 12#.

(2) No matter the output of the voltages from electric field was 5 V, 12 V, or 24 V, the crystal amount distributions are not uniform. It was until after pipe 4# did the crystal distribution present the tendency of being first stable and then small increment.

(3) With the output pressure of 12 V and 24 V, the pipe crystal axial distribution curves run in identical directions, and crystal amounts were almost identical, and their variation with voltage was not notable. Under output voltage of 5 V, the crystal amounts of all pipes were all less than that under the two electric field patterns.

The crystal amount of pipe under a 5 V electric field is less than that under 12 V and 24 V. Hence, the axial distribution curves of two electric field patterns under voltage 5 V were compared. The crystal axial distribution curves of circumferential and parallel plate electric fields are shown in Figure 17.

The figures show that under the condition of a 5 V electric field, the axial distribution curves of these two electric field patterns are roughly identical. However, the circumferential field of pipes exceeding pipe 5# keeps stable, while the parallel electric field of pipes exceeding pipe 4# remains relatively

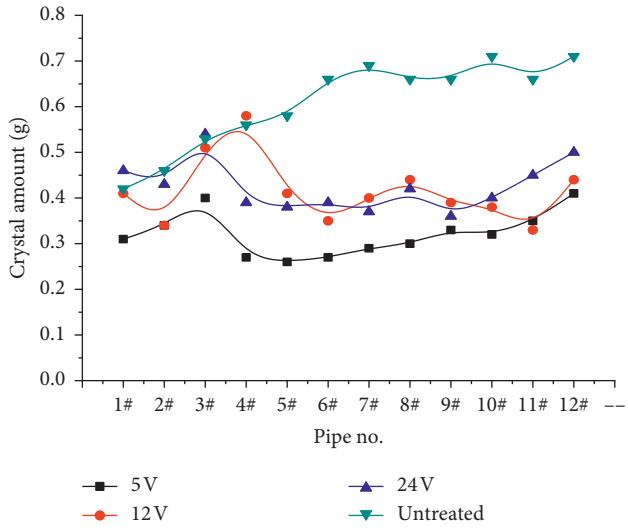

Figure 16: Parallel electric field mode and corresponding group pipe axial distribution curves.

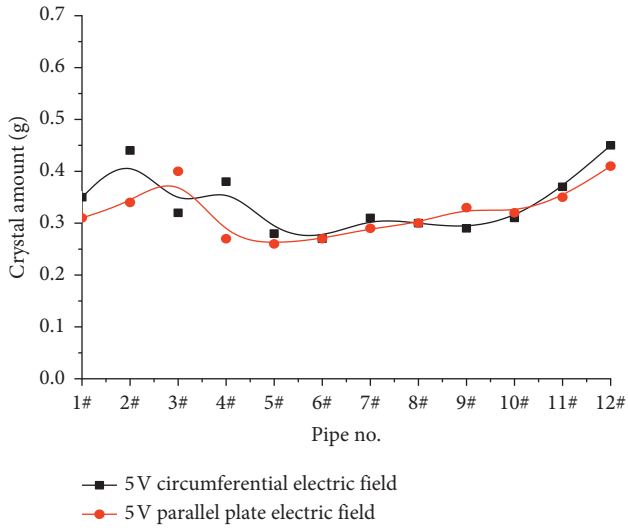

Figure 17: Contrast of circumferential electric field under 5 V and parallel plate electric field mode axial distribution curves.

stable. Under circumferential field condition, the crystal amounts at the ends of the pipe are relatively larger that is vulnerable to blockage, and pipe crystal amount fluctuates considerably. Hence, the parallel plate electric field pattern can be chosen to be imposed on the bottom and the top of drainage pipes of tunnels to resist scale.

3.2. Impact of Electric Fields on Scale Inhibition of Drainage Pipes of Full Flow. The impacts of electric fields on crystallization in drainage pipes of tunnels are mainly analyzed from the three aspects: crystal amount, crystallizing speed, and scale resistance rate so as to judge the scale resistance effect of the electric fields. The two electric field patterns, the circumferential and parallel plate electric fields, are compared and contrasted comprehensively, and relative scale resistance measures are proposed. The test results are shown in Table 4.

3.2.1. Impact of Electric Fields on Crystal Amounts. In the analysis of the impact of electric fields on crystal amount, the crystal amount in the pipes that have been in operation for 50 days were chosen for comparison and analysis. Table 4 shows that after the pipe was imposed with the circumferential electric field of 5 V for 50 days, the crystal amount in the pipe is minimum in value of 3.85 g. After the pipes without electric field ran for 50 days, the crystal amount was up to 7.3 g in value that was much higher than the crystal amount with static electric field treatment.

In order to understand the increment of crystal amount, the curves indicating the progressive increase of pipe crystal amount along with running period of circumferential and parallel plate electric fields are hereby plotted as shown in Figures 18 and 19.

Figures 18 and 19 indicate the following:

(1) After the drainage pipes go through the circumferential electric field and parallel plate electric field treatment, the amount of crystal in them is reduced considerably.

(2) Under the three voltages: 5 V, 12 V, and 24 V, the crystal amount is minimum in the pipe under 5 V and maximum in the pipe under 24 V.

(3) With the increase of running time, the crystal amount in the pipes through electric field treatment changes and increases in a linear manner but falls back in the later period. However, the increase rate of the crystal amount in the ordinary pipes without electric field treatment decreases progressively, and after 40 to 50 days in operation, the crystal amount in the ordinary pipes declines that indicates the sign of falling-off of crystal substances. The crystal amount is decreasing the crystal amount in the pipes through electric field treatment maintained at lower level and the rate of increase was inclined to reduce.

To sum up the above, under the two patterns of circumferential and parallel plate electric field patterns, the difference in crystal amount in the two pipes was small. However, in the 5 V electric field, the crystal amount of parallel electric field was lower than that of circumferential field and maintained at the lowest level from the view of crystal amount comparison. Hence, it can be concluded that the parallel plate electric field pattern is superior to the circumferential electric field pattern.

3.2.2. Impact of Electric Field on Crystallizing Speed. According to the above mentioned equation, calculation, crystallizing speed of crystallizing rate was plotted as shown in Figures 20 and 21.

Figures 20 and 21 indicate the following:

(1) No matter whether electric fields are imposed, the crystallizing speed was inclined to decrease with the increase of the running time and maintained a magnitude level of 10^{-2} in the later period.

(2) After going through treatment of circumferential and parallel plate electric fields, the declining time of

Table 4: Summary of test data of the total amount of crystals in pipes of different running cycles under different electric field modes.

Electric field mode / Running time	Voltage value (V)	Total crystal amount in pipes				
		10 d	20 d	30 d	40 d	50 d
Circumferential electric field	5	1.86	2.31	2.83	3.72	4.07
	12	2.13	2.77	3.52	4.14	4.38
	24	2.78	3.23	3.82	4.48	4.93
Parallel plate electric field	5	1.99	2.61	3.12	3.72	3.85
	12	2.22	2.88	3.7	4.43	4.98
	24	2.09	3.09	3.97	4.67	5.09
Contrast groups		3.27	5.43	6.52	7.41	7.3

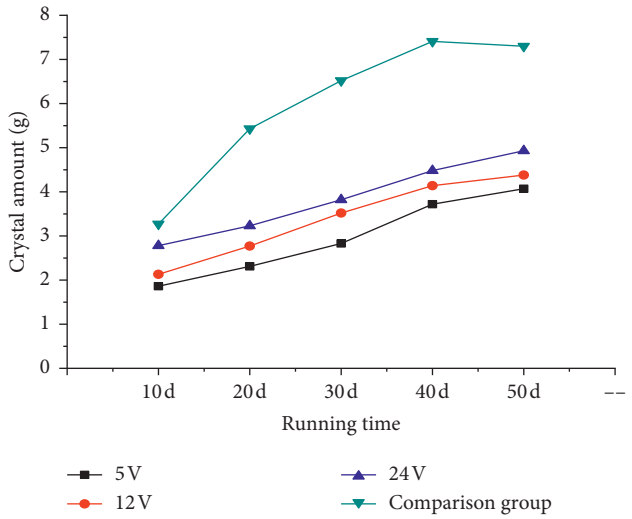

Figure 18: Curves indicating the progressive increase of crystal amount with the circumferential electric field.

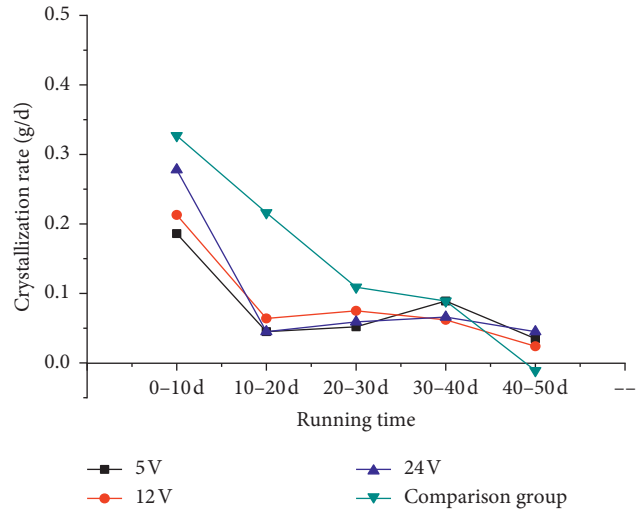

Figure 20: Curves indicating circumferential electric field crystallizing speed.

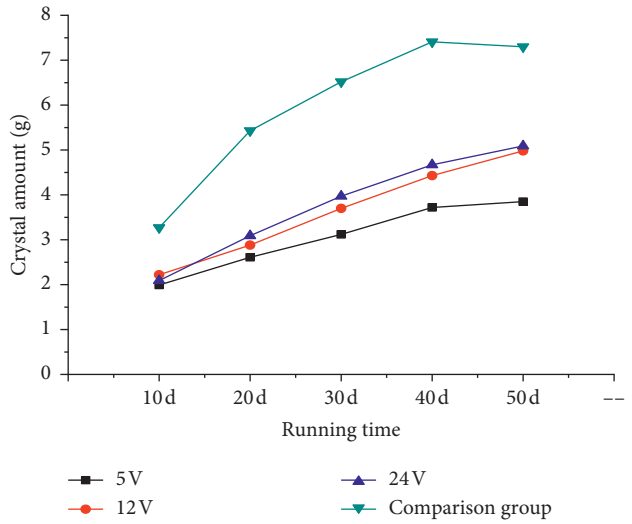

Figure 19: Curves indicating the progressive increase of crystal amount with a running period of the parallel plate electric field.

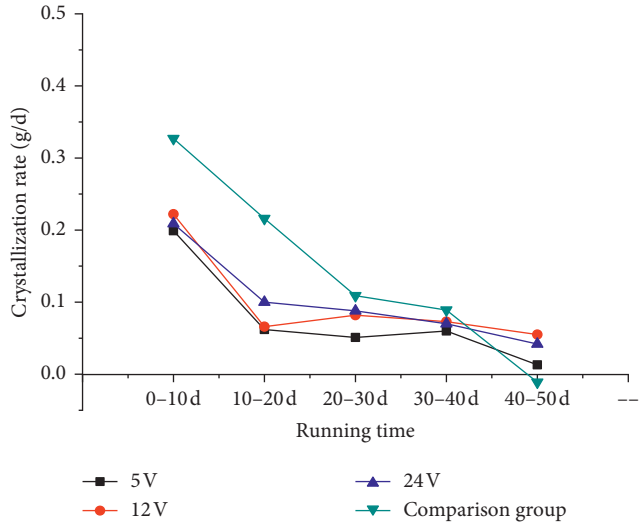

Figure 21: Curves indicating crystallizing speed under parallel plate electric field.

crystallization rate was much earlier, and the crystallization rate maintained a lower level. In the ordinary pipes that were running for around 20 days, the crystallization rate started to decline. It was concluded that electric fields effectively reduced the generation of crystalline materials.

(3) In the pipes without treatment within running period of 40 to 50 days, its crystallization rate declined

considerably with its crystallization rate of −0.011 g/d, which was lower.

(4) Under circumferential electric field pattern after the electric field under 12 V for 50 days, crystallization rate maintained a low level. Under parallel plate electric field pattern, after a 5 V electric field ran for 50 days, the crystallization rate maintained a low level.

Two different electric field patterns under similar electric fields are considered, and the crystallization rates are obtained as shown in Figures 22–24, which are compared and contrasted.

Figure 22 shows that in the early operation stage of the pipe, the crystallization rate of the parallel plate electric field of the output voltage of 5 V is higher than that of circumferential electric field mode. However, in the later stage, the crystallization rate of the parallel plate electric field is lower than that of the circumferential electric field. Since the crystallization rate of both types of electric fields in later period all kept the order of 10^{-2}, the difference is small.

Figure 23 shows that in the five running periods, the crystallization rate of parallel plate electric field under voltage 12 V is higher than that of circumferential electric field, and the rate difference is progressively increased. The crystallization rates of both patterns maintained a lower level.

Figure 24 indicates that in the early running stage of the pipe, the crystallization rate of the circumferential electric field under voltage 24 V is higher than that of parallel plate electric field, but in the later stage, the crystallization rate of circumferential electric field declined faster and, at last, was almost same as the crystallization rate of parallel electric rate.

To sum up, the above crystallization rates of both circumferential electric field and parallel plate electric field patterns present the law of faster crystallization in the early stage and keeping the level of 10^{-2} in the later stage, and the difference is small.

3.2.3. Impact of Electric Field on Scale Inhibition Rate. By the abovementioned calculation formula for scale inhibition rate, the scale inhibition rate of different electric field patterns under the effect of different voltages after running 50 days may be obtained as shown in Table 5.

The following conclusions can be obtained from Table 5:

(1) After going through the electric field for over 50 days, the scale resistance rate of circumferential field device with the output voltage of 24 V is 32.47% that is smaller, and the largest scale resistance rate under output voltage of 5 V is 44.25% that is the maximum. The scale resistance rate of parallel plate electric field device under output voltage of 24 V is 30.27% that is minimum, while the scale resistance rate under output voltage of 5 V is 47.26% that is maximum.

(2) Voltage value is of great impact on scale resistance rate. Within voltage range 5 V~24 V, the scale resistance rate declines with increase of voltage, and

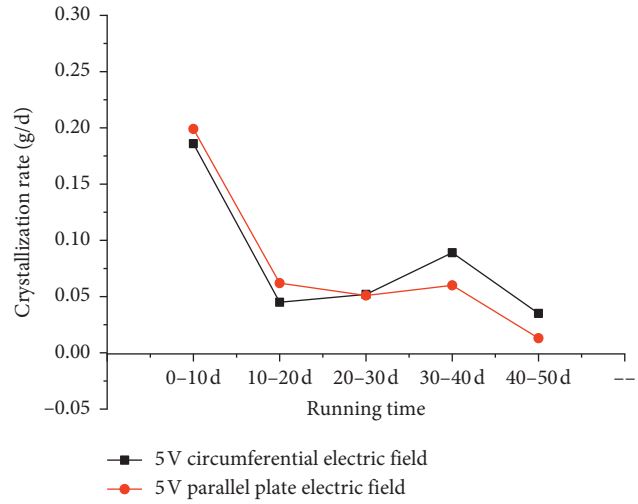

Figure 22: Crystallization rate comparison between 5 V circumferential electric field and parallel plate electric field.

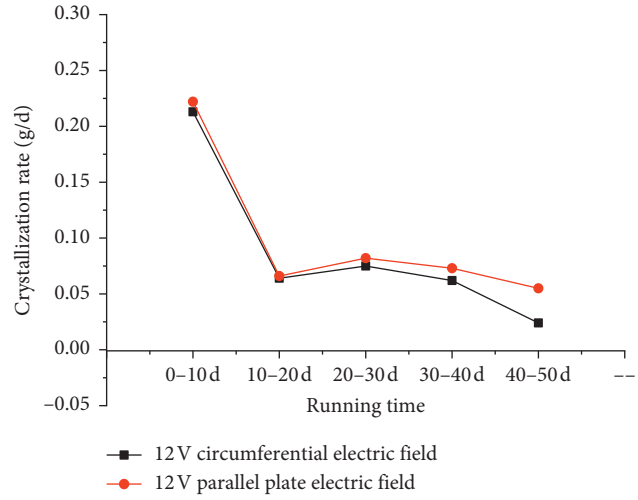

Figure 23: Contrast of crystallization rates between circumferential electric field and parallel plate electric field patterns.

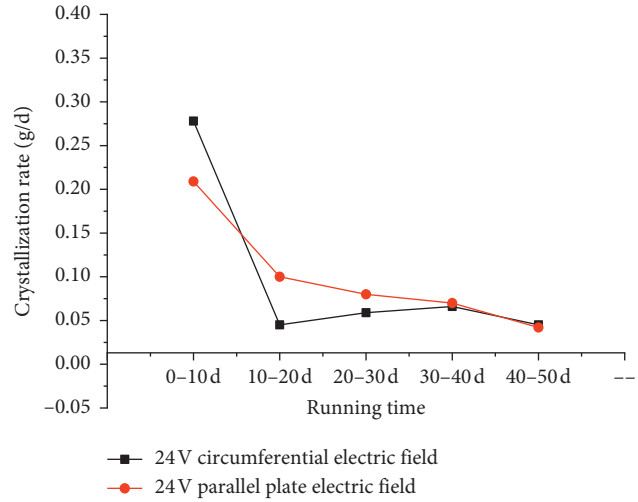

Figure 24: Contrast of crystallization rates of circumferential electric field and parallel pate electric fields under voltage 24 V.

Table 5: Contrast of scale inhibition rates circumferential electric field and parallel plate electric field patterns.

	Electric field pattern (V)	Scale inhibition rate (%)
5	Circumferential electric field	44.25
	Parallel plate electric field	47.26
12	Circumferential electric field	40.00
	Parallel plate electric field	31.78
24	Circumferential electric field	32.47
	Parallel plate electric field	30.27

under the condition of voltage 5 V, the scale resistance rate reaches the highest.

(3) Under the voltage 12 V and 24 V, the scale resistance rate has little difference. Then it is concluded that the scale resistance rate in this range of voltage has unnoticeable changes with variation of voltages.

To sum up the above, under the output voltage 5 V, the scale resistance rate of parallel plate electric field is superior to that of circumferential electric field pattern. While under the output voltages of 12 V and 24 V, the scale resistance rate of the circumferential electric field is superior to that of parallel plate electric field. The highest scale resistance rate was produced at output voltage 5 V by parallel plate electric field pattern. Specifically, the parallel plate electric field at output voltage 5 V applies to the tunnel drainage pipe in the full-flow state.

3.3. Impact of Electric Field on Scale Resistance Effect of Semi-Flow Drainage Pipe. In reality, tunnel drainage pipes do not always keep a full-flow state. In the following section of this paper, the impact of electric field on the descaling effect of tunnel drainage pipe of semi-flow is analyzed, and as the result of comparison of test results, the electric field pattern and field direction more suitable and applicable to the drainage pipe of semi-flow are selected. Figure 25 indicates the test devices and the descaling effect on semi-flow drainage pipe affected by the electric field.

By the abovementioned test scheme in the test process, the impact of voltage is not to be considered, and only the electric field pattern and field direction are to be tested. Different groups A, B, C, and D are to be tested according to electric field directions. To achieve uniform tests and reduce errors as much as possible, same pipe length of 120 cm is selected, and an output voltage of 12 V is adopted. After going through five test periods, namely, 50 days, the crystal amount in the pipes is obtained and shown in Table 6.

3.3.1. Impact of Electric Field on Crystal Amounts. After the test was running over 50 days, the crystal amount in the pipe treated with circumferential electric field is obviously more than that in the ordinary pipes untreated with the electric field. The crystal amount generated by means of attracting calcium ions at center in pipe of group A reaches up to 8.96 g that is the highest quantity. After the pipes are treated with a parallel plate electric field for 50 days, the crystal amount in the pipe is 7.01 g that is the lowest in quantity and is lower

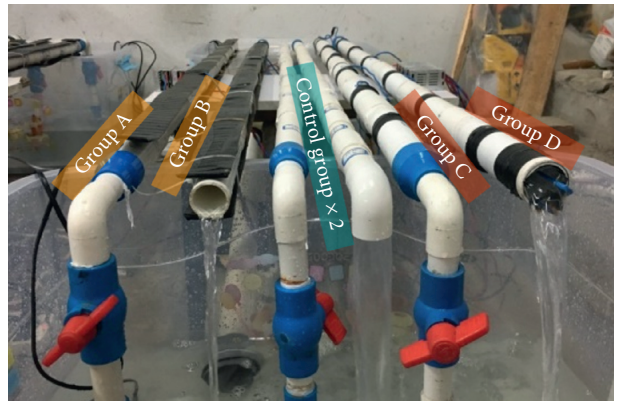

Figure 25: Test devices indicating descaling effect on semi-flow drainage pipe affected by the electric field.

Table 6: Summary of total crystal amount in the pipes within respective periods.

Electric field pattern	Field direction	Total crystal amount in pipes (g)				
Running time		10 d	20 d	30 d	40 d	50 d
Circumferential electric field	Group A	3.64	4.96	6.51	7.77	8.96
	Group B	3.01	4.49	5.85	7.07	7.94
Parallel plate electric field	Group C	5.66	7.38	8.77	8.54	7.01
	Group D	5.14	6.96	8.13	8.84	7.55
Comparison group		2.77	5.02	6.51	7.75	7.47

than the crystal amount in the ordinary pipes untreated with the electric field. Hence, it is concluded that this electric field pattern is more applicable to the semi-flow tunnel drainage pipes.

In order to understand the increment of crystal amount, the tunnel crystal amount curves indicating crystal increasing progressively with the increase of running period are hereby plotted as shown in Figures 26 and 27.

The above figures indicate that the crystal amount in pipes improved by circumferential electric field increases in a linear manner with increase of time, while in the parallel electric field pattern and in ordinary pipes untreated with any electric field, the crystal amount increases in the early stage and then decreases in the later stage. The crystal amount decreased to a large degree in the pipes treated with the electric field, which indicates that under the electric field pattern, the adhesion of crystal on the inner wall of the pipe decreases, while in the ordinary pipes untreated with the electric field, the crystal amount decreases due to its falling-off in later stage.

To sum up the above analysis, the crystal amount is the lowest in quantity when the field lines are arranged in the direction from top to bottom in the parallel plate electric field, namely, calcium ions moving toward the lower semi-ring of the pipe. In terms of crystal amount, only this pattern is more suitable for semi-flow tunnel drainage pipes.

3.3.2. Impact of Electric Field on Crystallization Rate. According to the formula mentioned above, the crystallization rates of the four group test pipe sections are

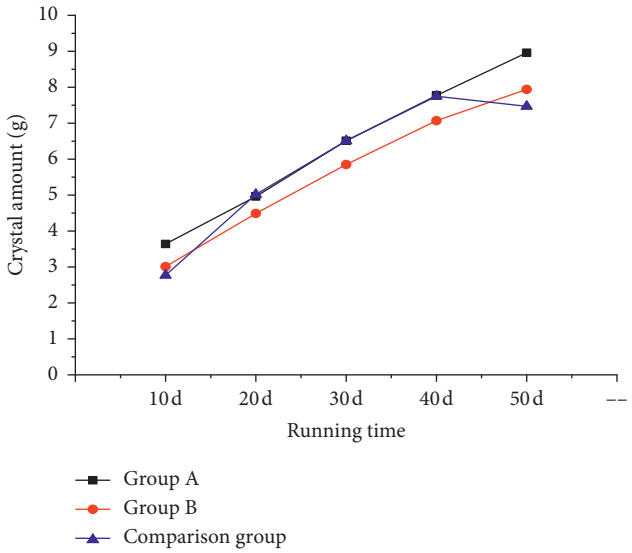

Figure 26: Curves indicating crystal amount variation with the increase of running period in the pipes improved with the circumferential electric field.

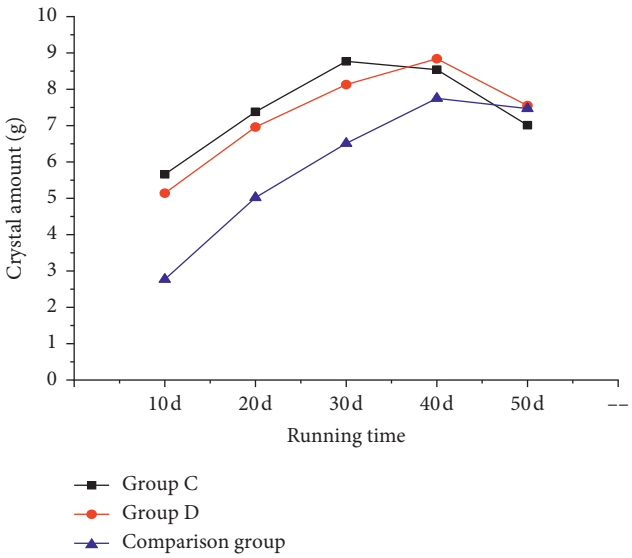

Figure 27: Curves indicating crystal amount variation with the increase of running period in the pipes improved with parallel plate electric field.

calculated, and the results of the calculation are shown in Figure 28.

Figure 28 indicates that under semi-flow conditions within the early 10 days of pipe running, the crystallization rate of the circumferential electric field was higher but decreased by a big margin after running for 10~20 days, then started keeping a lower rate but still keeping positive values, which indicated that the crystallization amount was still increasing. On the contrary, the crystallization rate of parallel plate electric field was highest in early 10 days, then declined in the large margin after running for 10~20 days, and became negative value after running for 30~40 days, which indicated that in course of crystallization, the crystals

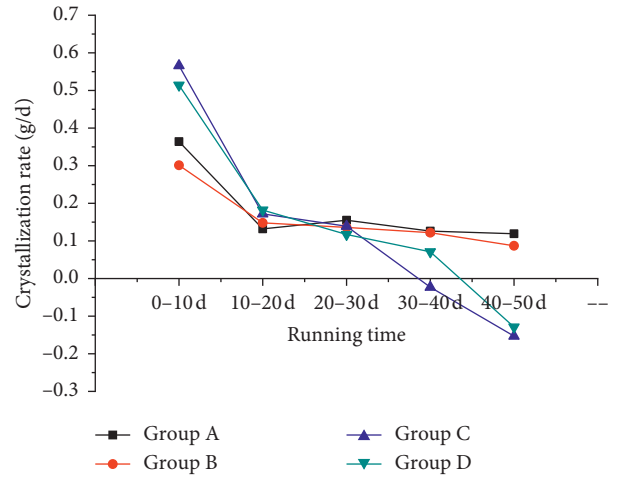

Figure 28: Curves indicating comparison of crystallization rate between circumferential electric field and parallel plate electric field (plus original).

started falling off in the later period. The crystallization rate of the pipes that are untreated by electric fields was not declining until 30~40 days or later.

Hence, by crystallization rate analysis in parallel plate electric field pattern, the crystallization rate in the early stage was fast but declined progressive in the later stage athatnd presented sign of falling-off of crystalline materials. The crystallization law was similar to those ordinary pipes without any electric field treatment, for the crystalline material did not adhere to the wall of pipe tightly. From crystallization rate, it is clear that the parallel plate electric field pattern is more applicable to the semi-flow tunnel drainage pipes.

3.3.3. Impact of Electric Field on Descaling Rate. The scale resistance rates of groups are shown in Table 7.

Table 7 indicates that all the groups except for group C showed negative values that indicated that in this given type of electric field, the crystallization amount of pipes are larger than that of ordinary pipes without electric field treatment. Hence, under parallel plate electric field pattern when the electric field lines are running from top to bottom scale, resistance effect can be achieved with scale resistance rate of 6.16% that is not ideal.

To sum up the above, parallel electric field pattern with field lines running from top to bottom is more applicable to tunnel drainage pipes in a semi-flow state.

3.4. Impact of Electric Field on Crystal Morphology. The conclusions of the above analysis are drawn from the test data gained. However, in order to explore the crystal form and type, crystal morphology and observe crystal combinations of crystalline materials in the pipes through electric field treatment scanning electron microscope (SEM) was conducted to the crystalline materials in the pipe in the test. The samples for scanning were taken from the easily cut samples of sound test effect, the pipes through parallel plate

Table 7: Contrasting the scale resistance rates between circumferential electric field and parallel plate electric field.

Electric field pattern		Scale resistance rate
Circumferential electric field	Group A	−19.95%
	Group B	−6.29%
Parallel plate electric field	Group C	6.16%
	Group D	−1.07%

electric field treatment, and the ordinary PVC pipes without electric field treatment. The photos of SEM that are enlarged by 200 times by scanning electron microscope are shown in Figure 29, and SEM photos that are enlarged by 5,000 times are shown in Figure 30.

The SEM photos that are enlarged by 200 times show the overall distribution of crystals. Figure 28 shows that crystals, although tightly arranged, presented cracking signs. After going through electric field treatment, the crystal material on pipe walls are thinner than the crystalline materials in the pipes untreated with the electric field. After going through electric field treatment, local falling-off of partial crystals in the pipe is notable, and crystals on the wall of pipe untreated with electric field are of nonuniform thickness in partial locations, and some locations are cellular, but the crystalline materials are dense.

After overall analysis of crystal forms and crystal morphology, it can be obtained that through electric field treatment, the adhesion between crystal and pipe wall is poor, and cracking or falling-off appears that indicates that the electric field effect can be effective on scale resistance and scale prevention in a certain degree.

After electric field treatment, the morphology of the crystals adhered to the internal wall of pipes presents an irregular pattern, and the crystal surface is worn out, loose, and porous. The crystalline material in the pipe untreated with electric field presents regular hexahedrons that are densely arranged.

To sum up the above, through treatment of electric field, the binding strength between the pipe wall and crystals may decrease, and the crystals may show a state of looseness and porousness. Hence, the electric field may cause a decrease in crystal weight in the pipe and be effective on scale prevention and resistance.

4. Discussion

4.1. Axial Distribution Law in Circumferential Electric Field Pattern. The production of the above signs has the following causes:

(1) The primary reasons for the generation of nonuniform crystals at fore-end of the tunnel are following: after the ions in the water enter the pipe, the movement of the ions increases under the effect of the electric field, and the cation and anion collide more frequently that causes more crystals gathering at fore-end of the pipes. In addition, due to the fact that 90° elbow was used in the water inlet of the pipe in the test, flow turbulence is generated, thus increasing the probability of crystal core generation.

(2) The main cause of little differences in crystal amount in pipes 1# and 2# lies in that when water flow enters inside pipe treated with the electric field, the effect generated by the electric field is not stable, and the movement of ions is subject to greater impact of water flow variation.

(3) The crystal amount at intermediate positions inside pipes keeps relatively stable, and the main cause is that the electric field has already discrete cation and anion causing the smaller probability of the contact between the cation and anion. Thus, the crystal amount keeps relatively stable.

(4) In the pipe outlet section, all the four axial distribution curves increase. The main cause is that in the test process, the pipe outlet is not isolated from air; specifically, the pipe outlet section is exposed to air and contacts with CO_2 and is vulnerable to the impact of the external environment.Therefore, the crystal amounts increase.

To better elaborate the nonuniform section and stable section in the axial direction of the pipe, the ion distribution in the pipe treated with the circumferential electric field can be plotted by the rough distribution of ions as shown in Figure 31. In this figure, the fore part is one where a large amount of ions collided under the effect of the electric field, and the probability of forming crystal cores is increased. Meanwhile, under the effect of current, crystal core moves and forms crystal, thus causing nonuniformness. However, in the rear part of the pipe, the ions are separated, and the probability of forming crystals is reduced. Therefore, the crystal amount is relatively stable.

4.2. Law of Axial Distribution in Parallel Plate Electric Field Pattern. The abovementioned signs are caused by the following causes:

(1) The crystal amount fluctuated in the fore part of the pipe mainly due to the cause that after the ion in water entered the pipe, the movement of ions increased under the effect of the electric field, thus increasing the probability of collision between cation and anion that further causes larger amount of crystal deposited in the fore part of the pipe. In addition, since the 90° elbow joint was used at the inlet of pipe in the test, the water flow entered the tested pipe from the water pump, and the water flow changed abruptly, and flow turbulence was generated, thus increasing the probability of crystal core generation.

(2) In the middle and outlet sections of the pipe, the distribution law of the crystal amount and its causes are the same as the above, which are not repeated here.

(3) Under the voltage of 5 V, the less collision between calcium ions and the wall of the pipe happened, and crystalline materials cannot easily and tightly adhere to the wall of the pipe. However, compared with the

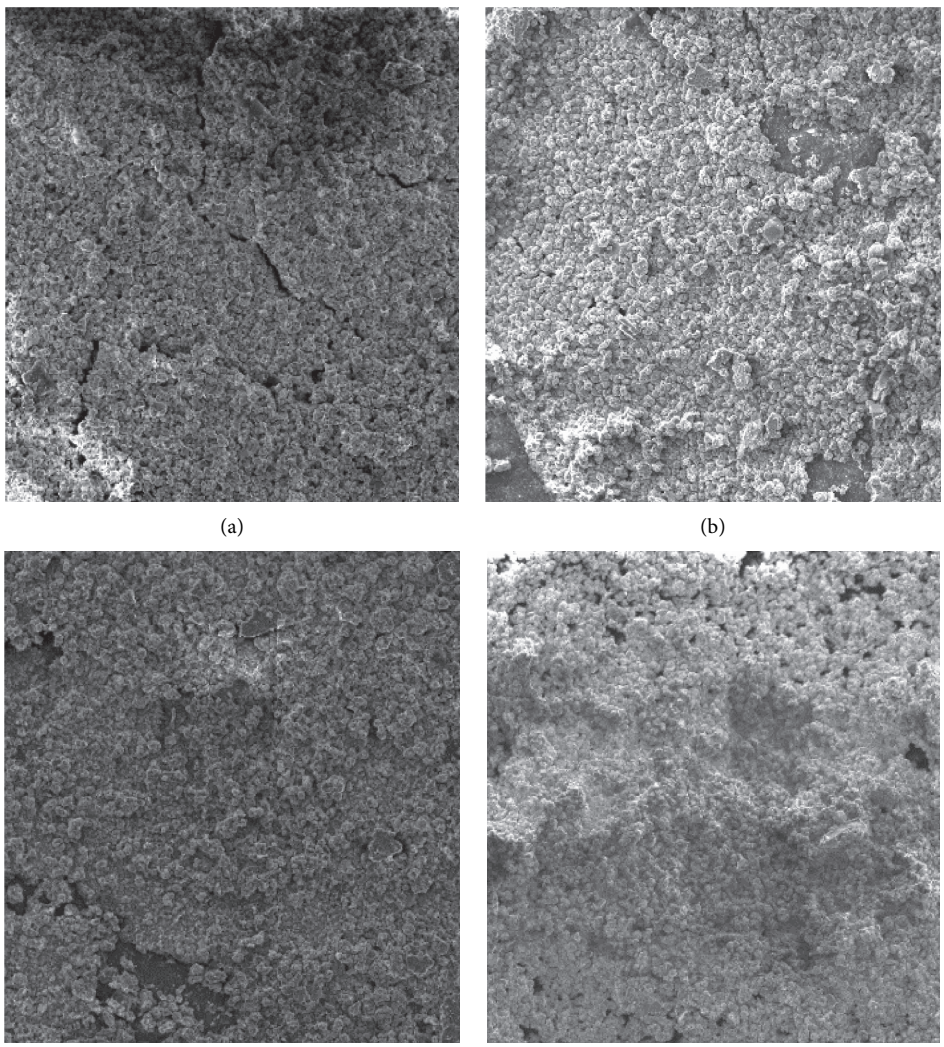

(a) (b)

(c) (d)

Figure 29: SEM photos of pipe crystals treated with the electric field: (a) 5 V parallel electric field; (b) 12 V parallel electric field; (c) 24 V parallel plate electric field; and (d) untreated.

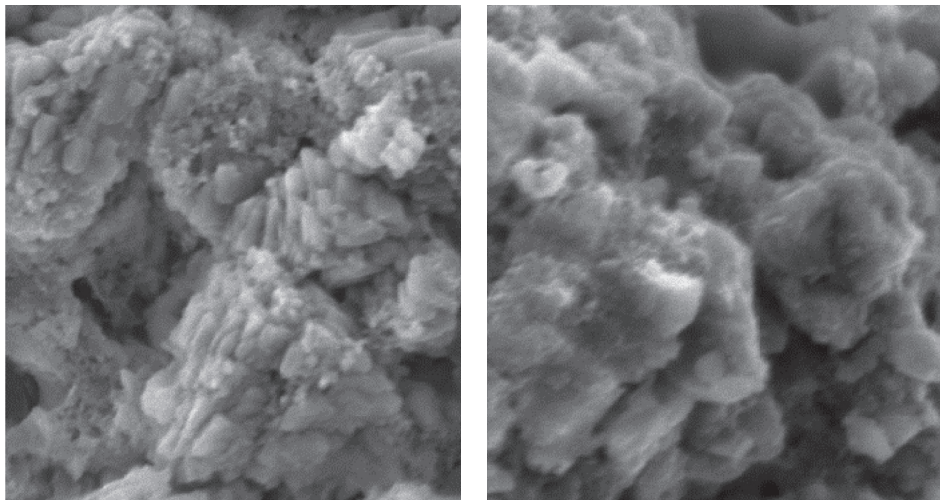

(a) (b)

Figure 30: Continued.

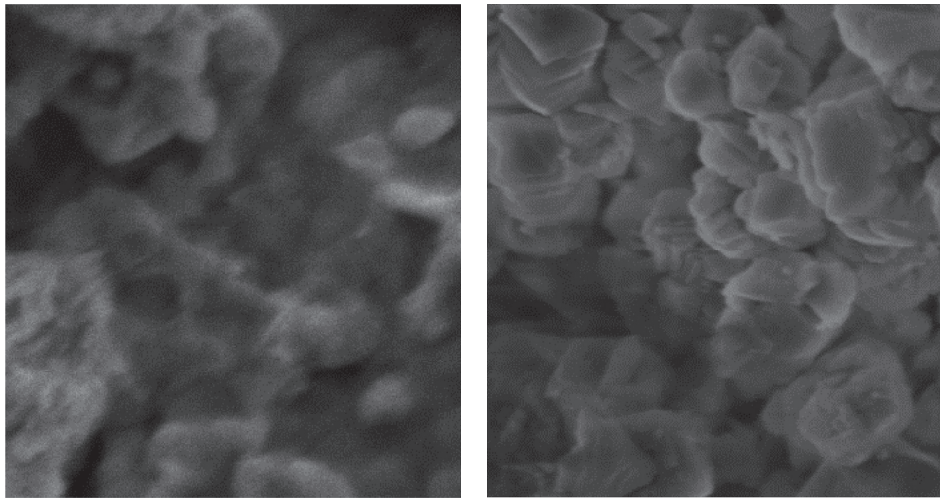

(c) (d)

Figure 30: SEM photos of crystals in pipes treated with the electric field: (a) 5 V parallel plate electric field; (b) 12 V parallel electric field; (c) 24 V parallel plate electric field; and (d) untreated with the electric field.

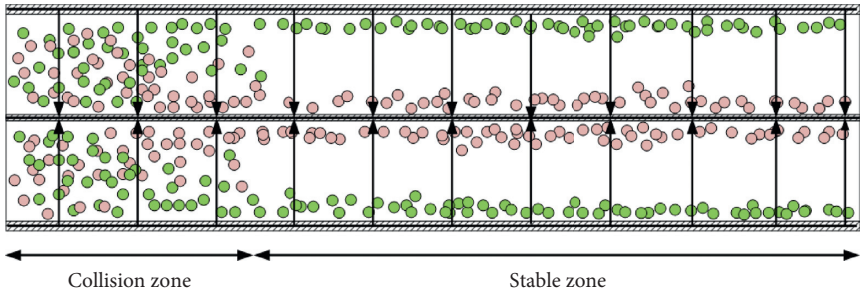

Figure 31: Schematic sketch indicating ion distribution in the pipes improved by the circumferential electric field.

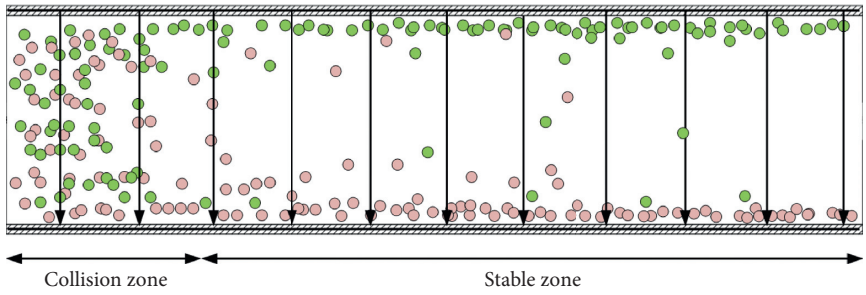

Figure 32: Schematic figure of ions distribution in pipes of parallel plate electric field.

circumferential electric field, the parallel plate electric field pattern is subject to little impact of voltage.

The ion distribution in the pipe treated with a parallel plate electric field is indicated in Figure 32. In the fore part of the pipe, ions collided, and under the effect of the electric field, frequent collision causes the greater probability of crystal cores. Meanwhile, under the effect of water current, the crystal core moved and formed crystals, thus causing nonuniformness. However, in the rear part of the pipe, ions were separated that causes a lower probability of forming crystal cores, and the crystal amount maintained stable.

5. Conclusions

In this paper, a study is conducted to solve the problems of pipe blockage of crystals in tunnel drainage pipes in hard water areas. Two types of electric field devices imposed on tunnel drainage pipes are designed, and the study is carried out on the law of crystalline material axial distribution in the tunnel drainage pipes under these two electric field patterns.

In addition, the scale resistance effects of electric field patterns are compared and analyzed. The main results of the study are shown as follows:

(1) Two test devices that impact crystallization in tunnel pipes are designed, which are circumferential and parallel plate electric field devices.

(2) By analyzing the results of laboratory tests on the law of tunnel crystal axial distribution, it is concluded that in the ordinary pipes untreated by electric field, the crystal amount increases progressively along axial direction under the condition of semi-flow, and the crystal amount keeps relatively uniform in later half-section. In the pipes treated with the circumferential and parallel plate electric fields, the crystal amount fluctuates in the early stage and then stabilizes in water flow direction with crystal amount higher in fluctuating section and less in uniform section, and its uniform section is longer than that of ordinary pipes.

(3) It can be concluded from laboratory test on the scale resisting effect of pipe with full flow imposed with the electric field that no matter electric field is imposed, or crystallization rate did not increase with the running time and are all inclined to decrease. However, with the effect of electric fields, crystallization rate acceleration is decreased to some level to enable the crystallization rate to maintain a level of 10^{-2}.

(4) In combination with the test results of scale resistance effect of full- and semi-flow pipes imposed with electric fields, it can be concluded that different electric field pattern generates different scale resistance effects. With a full-flow pipe, the parallel plate electric field of the output voltage of 5 V presents a better effect with the scale resistance rate of 47.25%. With semi-flow pipe, the parallel plate electric field pattern with field lines arranged in the direction from top to bottom presents a better scale resistance effect with a resistance rate of 6.16%.

(5) SEM indicates that with the effect of electric field, the external shape of calcium carbonate crystal may change. Without an electric field imposed, the calcium carbonate crystal presents hexahedron in the tight arrangement. After the electric field is imposed, calcium carbonate crystal is worn out on the surface, porous in crystal structure, and loose.

Data Availability

The data used to support the findings of this study are available from the corresponding author upon request.

Conflicts of Interest

The authors declare that they have no conflicts of interest.

Acknowledgments

This work was supported by the National Natural Science Foundation of China (No. 51708070), Chongqing Science and Technology Commission (cstc2017jcyjAX0056), and Sichuan Railway Investment Group Co., Ltd. (SRIG2019GG0004).

References

[1] J. Zhuge, S. Zhang, Y. Han et al., "Super fine calcium carbonate crystallization process and composition of super fine calcium carbonate of different morphology," *Chemical Studies*, vol. 9, no. 3, pp. 26–30, 1998.

[2] M. Luo and Z. Lu, "Dynamic study on calcium carbonate crystallization process," *Fine Chemical Engineering*, vol. 17, no. 8, pp. 463–466, 2000.

[3] R. Xiao, J. Zhou, J. Pan et al., "Scaling mechanism and model prediction of oilfield water line," *Oil-Gasfield Surface Engineering*, vol. 32, no. 3, pp. 20-21, 2013.

[4] O. J. G. Vetter, "How barium sulfate is formed: an interpretation," *Journal of Petroleum Technology*, vol. 27, no. 12, pp. 1515–1524, 1975.

[5] J. Moghadasi, M. Jamialahmadi, H. Müller-Steinhagen, and A. Sharif, "Scale formation in oil reservoir and production equipment during water injection (kinetics of $CaSO_4$and $CaCO_3$crystal growth and effect on formation damage)," in *Proceedings of the SPE European Formation Damage Conference Society of Petroleum Engineers*, Hague, Netherlands, December 2003.

[6] J. Moghadasi, M. Jamialahmadi, H. Müller-Steinhagen, and A. Sharif, "Formation damage due to scale formation in porous media resulting from water injection," in *Proceedings of the SPE International Symposium and Exhibition on Formation Damage Control*, Society of Petroleum Engineers, Lafayette, Louisiana, February 2004.

[7] L. Tore, M. Lioliou, T. Ostvold, L. O. Josang, and P. Randhol, "Kinetics of $CaCO_3$scale formation during core flooding," in *Proceedings of the SPE International Oilfield Scale Conference*, SPE114045, Aberdeen, UK, May 2008.

[8] B.-L. Salima, T. V. Charpentier, A. Neville et al., "Evaluation of anti-fouling surfaces for prevention of mineral scaling in sub-surface safety valves," in *Proceedings of the SPE International Oilfield Scale Conference and Exhibition*, Aberdeen, Scotland, May 2014.

[9] H. A. Viles and A. S. Goudie, "Tufas, travertines and allied carbonate deposits," *Progress in Physical Geography: Earth and Environment*, vol. 14, no. 1, pp. 19–41, 1990.

[10] G. Lu, "Hydrogeochemical study on the genesis of cold-water travertine in Huanglong-Jiuzai natural reserve in Sichuan," *Journal of Mineralogy and Petrology*, vol. 14, no. 3, pp. 71–78, 1994.

[11] Y. Yang and B. W. Guangxi, "Hot spring formation and evolution and carbonization deposits mechanism study," Master Degree Dissertation, China University of Geosciences, Beijing, China, 2006.

[12] Y. Tang, "Study on elimination of water hardness in Weibei Karst regions," Master Degree Dissertation, Chang'an University, Xi'an, China, 2014.

[13] Q. Chen, "Experimental study on the effect of fluoride and aluminum impurity ions and organic acid additives on the crystallization process of desulfurized gypsum," Master Degree Dissertation, Xiangtan University, Xiangtan, China, 2014.

[14] R. Chen and L. Hu, "Application of XSG-4 model water treatment machine in scale prevention and resistance in tower typed distiller," *Journal of Shengyang Pharm University*, vol. 8, no. 4, pp. 79-80, 1991.

[15] Y. Xue, "The problem of scale prevention and descaling the ash water pipe system of the thermal power plants has been thoroughly solved," *Industrial Water Treatment*, vol. 20, no. 5, p. 30, 2000.

[16] C. Wang, Z. Quan, Y. Chen et al., "Experimental study on anti-scaling performance of high-voltage electrostatic field," *Journal of Engineering Thermophysics*, vol. 28, no. 6, pp. 1028–1030, 2007.

[17] H. Li, Z. Liu, Y. Gao et al., "Impact static electric field on $CaCO_3$crystallization process and joint performance of green descaling agents," *Journal of Chemical Engineering*, vol. 64, no. 5, pp. 1736–1742, 2013.

[18] H. Li, Z. Liu, Y. Gao et al., "Impact of high voltage static electric field on descaling performance of green descaling agent and water scale forms," *Water Treatment Technology*, vol. 39, no. 4, pp. 24–27, 2013.

[19] X. Wu, Z. Liu, H. Li et al., "Synergistic scale inhibition of itaconic acid homopolymer and high voltage electrostatic field," *Industrial Water Treatment*, vol. 30, no. 5, pp. 33–35, 2010.

[20] D. F. Wang, L. B. Huang, M. M. Wei et al., "MD simulation of influence of high voltage static electric field on crystallization of calcium carbonate," *Industrial Water & Wastewater*, vol. 113, pp. 255–264, 2010.

[21] H. H. Li, Z. F. Liu, X. Li et al., "Effect of electrostatic field on calcium carbonate precipitation," in *Proceedings of the 2011 5th International Conference on Bioinformatics and Biomedical Engineering, (iCBBE)*, pp. 1–4, IEEE, Wuhan, China, May 2011.

[22] Z. Li, J. Zhao, J. Zhao et al., "Analysis of electric field distribution in high voltage electrostatic water processor and study of scale inhibition effect," *Proceedings of CSEE*, vol. 34, no. 35, pp. 6296–6303, 2014.

[23] J. I. Yuan and Y. Cui, "Experimental study on electronic water treating machine application conditions," *Taiyuan University of Technology*, vol. 31, no. 6, pp. 714–718+728, 2000.

[24] T. Cai, "Test study on high frequency electric field water treatment," *Water treatment technology*, vol. 23, no. 4, pp. 222–225, 1997.

[25] M. Li, Z. Peng, X. Nie, Q. Chen, and Q. Zhu, "Study on descaling performance of electronic water processor," *Water Supply and Drainage*, vol. 25, no. 1, p. 40, 1999.

[26] Y. Wang, *Study on Impact of Water Flow Speed Variation under Effect of Static Electric Field on Descaling Effect of Power Plant Circulating Water*, Inner Mongol University of Technology, Mongolia, China, 2018.

[27] C. Rolf, "In situ determination of the apparent solubility produce of amorphous iron sulphide," *Applied Geochemistry*, vol. 9, pp. 379–386, 1994.

[28] J. Chen, *Development of Water Treatment Device with Alternating Magnetic Field and Experimental Study on Scale Inhibition and Removal*, Chongqing University, Chongqing, China, 2014.